Supporting Information for

Photochemical Chlorination of Graphene

Bo Li[†], Lin Zhou[†], Di Wu[†], Hailin Peng[†], Kai Yan, Yu Zhou, and Zhongfan Liu*

Center for Nanochemistry, Beijing National Laboratory for Molecular Sciences (BNLMS), State Key Laboratory for Structural Chemistry of Unstable and Stable Species, College of Chemistry and Molecular Engineering, Peking University, Beijing 100871, People's Republic of China.

[†]These authors contributed equally to this work.

Email: zfliu@pku.edu.cn

Part 1. Schematic illustration of home-built photochemical chlorination system

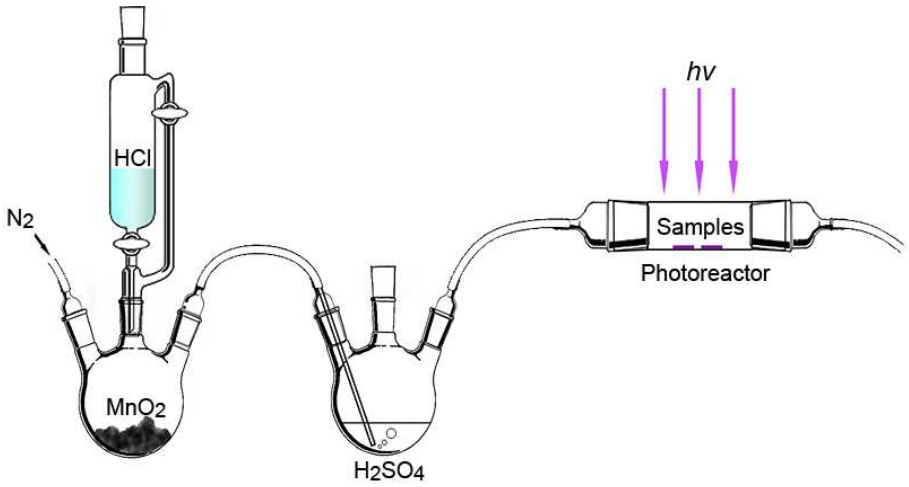

Figure S1. Schematic illustration of the home-built photochemical chlorination system.

Part 2. Characterizations of sufficiently photochlorinated graphene

After sufficient photochlorination (> 15 minutes of reaction), the single-layer graphene sheet became invisible under optical microscopy (Figure S2a). AFM images (Figures S2b-d) revealed that the

sufficiently photochlorinated graphene was broken into numerous nano-sized domains with lateral dimensions of 30~50 nm. Raman signal of the sufficiently photochlorinated graphene became very weak. As shown in Figure S2e, both D and G bands largely broaden while 2D peak completely disappears. In contrast, Raman intensity of the few-layer graphene flake adjacent to the single-layer graphene was much stronger upon the photochlorination. The prominent D and D' peaks of the few-layer sample emerged (Figure S2e). These observations suggested that few-layer graphene can also be photochlorinated with a relatively slow reaction rate.

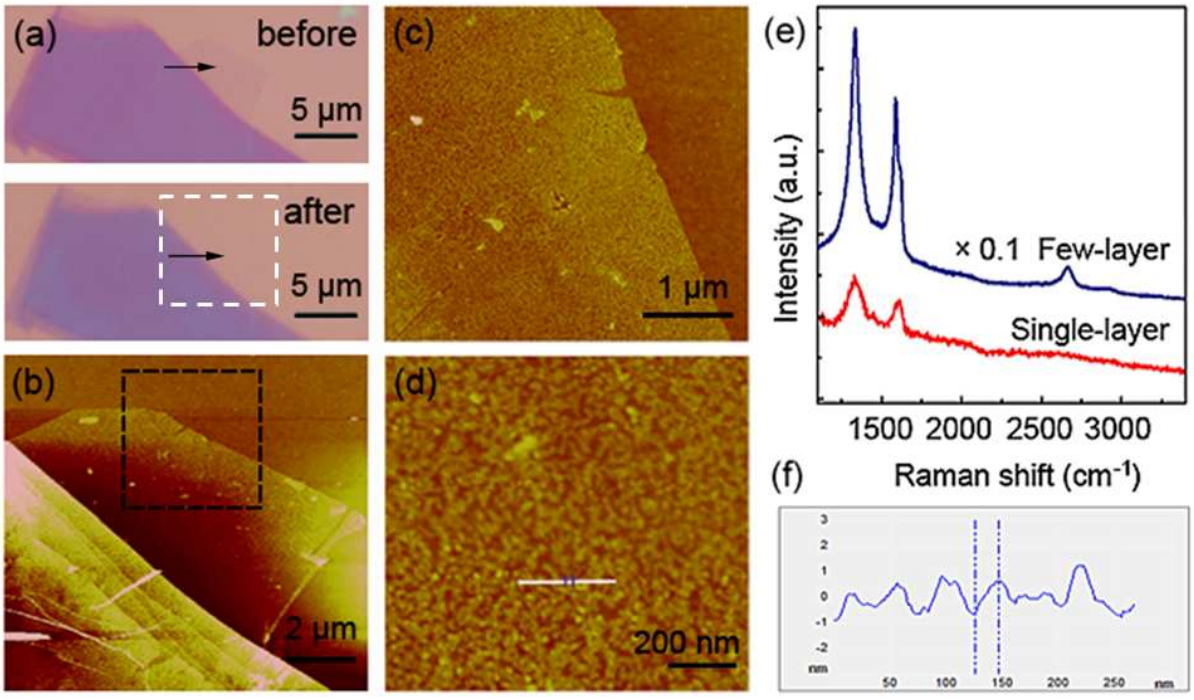

Figure S2. (a) Optical images of graphene flake before and after sufficient photochlorination. Single-layer graphene region is indicated by the black arrow. (b) AFM image of the graphene flake for an area of 10 × 10 μm^2 over the dashed white box area in (a). (c) AFM image of the photochlorinated single-layer graphene over the dashed box area in (b). (d) High-resolution AFM image of the photochlorinated single-layer graphene. (e) Raman spectra of the single-layer and the few-layer graphene as shown in (a) after sufficient photochlorination. (f) AFM profile along the white line in (d).

Part 3. Control experiment without the xenon lamp irradiation

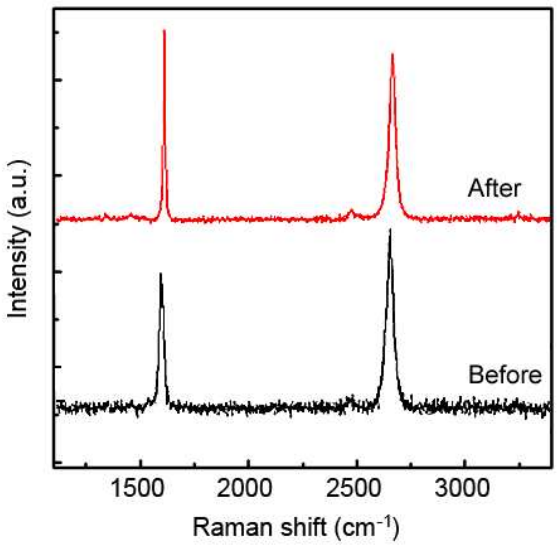

Figure S3. Raman spectra of a mechanically exfoliated single-layer graphene before and after exposed to chlorine for about 15 minutes without the xenon lamp irradiation.

Part 4. Reactivity of double-layer graphene

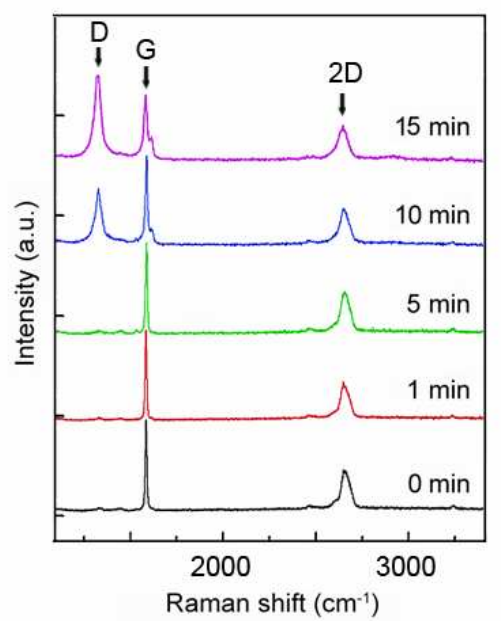

Figure S4. Time evolution of Raman spectra for double-layer graphene.

We observed that photochlorination reactivity of the double-layer graphene is significantly lower than the single-layer graphene, similar to the case for the photochemical reaction between benzoyl peroxide and graphene.[1] For example, the single-layer graphene developed a distinct D peak within 3 min (Figure 1b). Under the same reaction conditions, however, after 10 min of reaction the D peak appeared for the double-layer graphene (Figure S4).

Part 5. UV-Vis spectroscopy of photochlorinated graphene

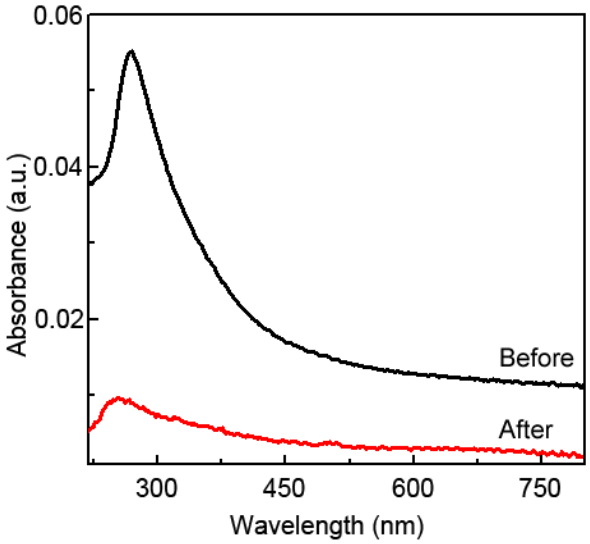

Figure S5. UV-Vis spectra of a CVD-grown graphene film on quartz substrate before and after photochlorination.

UV-Vis spectra of photochlorinated graphene were recorded on a Perkin Elmer Lambda 950 UV-Vis Spectrometer. Graphene films grown on copper foil were transferred onto quartz substrates for measurements. We obtained UV-Vis absorption spectra of the graphene before and after photochlorination (Figure S5), taking the same quartz substrate as the reference. The UV-Vis spectra presented a hypsochromic shift of λ_{max} and hypochromicity over the entire range after reaction. This

observation suggested that the π-conjugation system of the graphene basal plane was violently interrupted by covalently-bonded chlorine. It is inferred that the enhanced transparency of photochlorinated graphene is caused by the appearance of a band gap, similar to that of fluorinated graphene.[2]

Part 6. AFM image of the pristine graphene flake

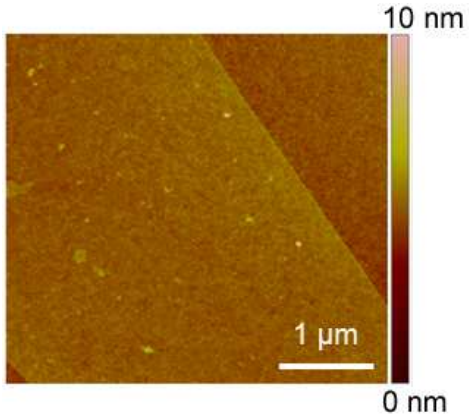

Figure S6. AFM image of the pristine graphene flake before photochlorination as shown in Figure 1 (c).

Part 7. Nondestructive, homogenous and patternable photochlorination

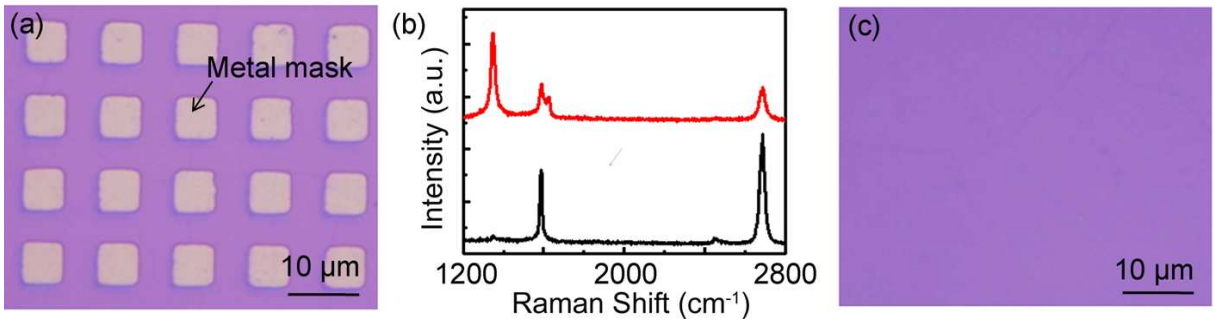

Figure S7. (a) Optical image of a CVD-grown graphene film on SiO_2/Si substrate covered with metal masks (10 nm Ti on 10 nm Al) deposited using electron-beam evaporation after photolithography. (b) Raman D band of the exposed region was obvious (red) while that of the masked region was negligible

(black). (c) Optical image of the graphene after 4 min photochlorination showing the nondestructive and homogenous features. The metal masks were removed by hydrochloric acid.

Part 8. XPS characterizations

XPS measurements were carried out using a Kratos Axis Ultra spectrometer with Al Kα monochromated X-ray at low pressures of 5×10^{-9} ~ 1×10^{-8} Torr. The large-area CVD-grown single-layer graphene films on Si/SiO_2 substrates were used for photochlorination and XPS characterization. The collection area was about 300×700 μm^2. The highest peak in C 1s spectra was shifted to 284.8 eV for charge correction.

As shown in Figure S8, chlorine peak is negligible for the graphene film before photochlorination. Two distinct peaks (Cl 2p and Cl 2s) appear after reaction, unequivocally indicating the presence of Cl. The XPS C 1s peak near 286.6 eV increases significantly, suggesting the formation of C-Cl bonds. From the high-resolution spectra of C 1s and Cl 2p (Figure 2a and 2b in main text), it can be concluded that the covalent bonds have been formed between Cl and graphene.

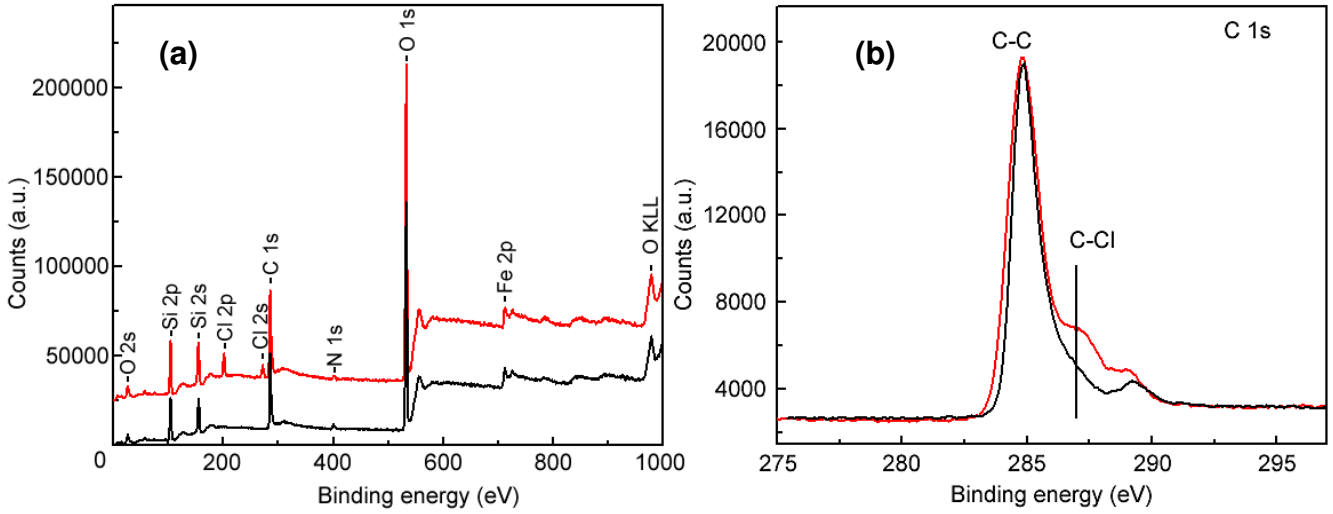

Figure S8. (a) XPS spectra of a CVD-grown graphene film transferred on Si/SiO_2 substrate before (black) and after photochlorination (red). (b) High-resolution C 1s spectra of CVD-grown graphene

films before (black) and after photochlorination (red).

Part 9. TEM and EDX studies

The photochlorinated graphene film was detached by etching the supporting SiO_2 substrate away with a dilute HF aqueous solution (~2 wt%) and subsequently transferred to Cu TEM grid with the assistance of a spin-coated PMMA film. The PMMA film was then removed by acetone. As shown in Figure S9 (b), the Cl signal was clearly detected by EDX, consistent with XPS data. The Cu peak may come from the Cu TEM grid. The Si and O peaks come from the SiO_2 residues after HF etching.

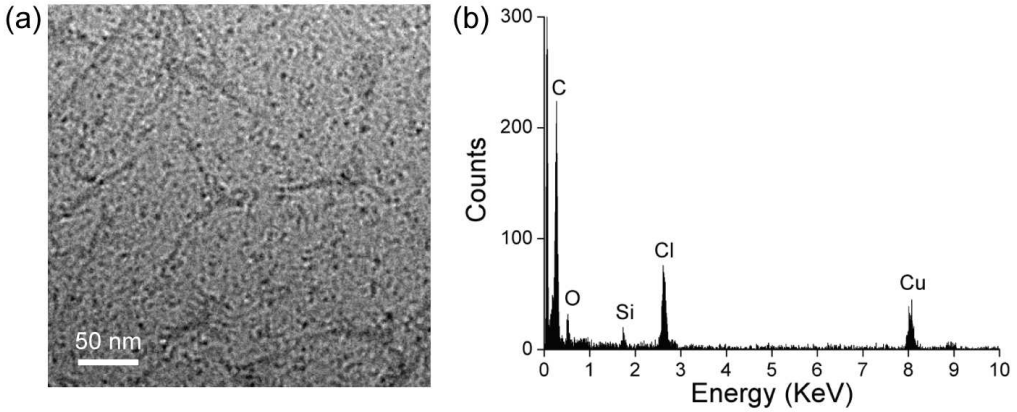

Figure S9. (a) TEM image of a photochlorinated graphene film. (b) EDX data of the photochlorinated graphene film.

References:

(1) Liu, H. T.; Ryu, S.; Chen, Z. Y.; Steigerwald, M. L.; Nuckolls, C.; Brus, L. E. *J. Am. Chem. Soc.* **2009**, *131*, 17099.

(2) Robinson, J. T.; Burgess, J. S.; Junkermeier, C. E.; Badescu, S. C.; Reineche, T. L.; Perkins, F. K.; Zalalutdniov, M. K.; Baldwin, J. W.; Culbertson, J. C.; Sheehan, P. E.; Snow, E. S. *Nano Lett.* **2010**, *10*, 3001.